Int J Clin Exp Med 2016;9(12):23345-23350
www.ijcem.com /ISSN:1940-5901/IJCEM0034124

Original Article

Ultrasound-induced microbubble cavitation promotes angiogenesis in ischemic skeletal muscle of diabetic mice

Ye Song[1], Xiaoyun Xie[2], Yuan Gao[3], Lingjing Jin[4], Peijun Wang[5]

Departments of [1]Ultrasound, [2]Geriatrics, [3]General Surgery, [4]Internal Medicine, [5]Radiology, Affiliated Tongji Hospital of Tongji University, Shanghai, China

Received June 21, 2016; Accepted October 30, 2016; Epub December 15, 2016; Published December 30, 2016

Abstract: Objective: This study aimed to investigate the effect of ultrasound-induced microbubble cavitation on the angiogenesis in ischemic skeletal muscle of diabetic mice and potential mechanism. Methods: Ischemia was induced in lower limb of db/db mice which were then randomly divided into four groups: control group, ultrasound group (US), microbubble group (MB) and US+MB group. After treatment, the ischemic skeletal muscle was collected for H&E staining. 7 days after treatment, RT-PCR and Western blot assay were performed to detect the expression of P-selectin, ICAM-1 and VEGF, and immunohistochemistry was done for VEGF expression in the skeletal muscle. Results: H&E staining showed there were a lot of red blood cells leaking into the skeletal muscle gap, the muscle fibers showed mild edema, and there was no myolysis in US+MB group. Immunohistochemistry showed VEGF expression in US+MB group was significantly higher than in remaining 3 groups, there were a lot of newly generated blood vessels, and the mRNA and protein expressions of VEGF, P-selectin and ICAM-1 were also markedly higher than in other groups. In control group, US group and MB group, a low VEGF expression was found, and RT-PCR and Western blot assay showed low expressions of VEGF, P-selectin and ICAM-1. Conclusion: Ultrasound-induced microbubble cavitation may cause mild damage to the endothelial cells of capillaries, resulting in transient inflammation in these endothelial cells, which may activate endothelial cells, up-regulate P-selectin and ICAM-1 expression, induce the secretion of endogenous VEGF and promote the angiogenesis in the lower limb.

Keywords: Ultrasound, microbubble, diabetes mellitus, angiogenesis, inflammation

Introduction

Diabetic peripheral artery disease (PAD) is one of severe chronic complications of diabetic mellitus (DM) and an important cause of disability, mortality and amputation, which significantly affects the quality of life of patients [1, 2]. Treatments for PAD mainly include surgery, pharmacotherapy and interventional therapy, but the efficacy is still poor in some patients. Therapeutic angiogenesis provides a new method for the therapy of ischemic vascular diseases, and targeted microbubble is becoming important in the diagnosis and therapy of ischemic diseases [3-5]. Some investigators intravenously injected albumin microbubble contrast agent and then ultrasound was used to detect the normal skeletal muscle [6]. They found congestive nutritional blood flow and newly generated arterioles, indicating that ultrasound may promote angiogenesis via disrupting the microbubbles and then improve the local blood flow. They also proposed that this may be used for the therapy of ischemic diseases. Ultrasound-induced microbubble cavitation may cause damage to the microvessels, which may induce angiogenesis and vascular remodeling. This may be ascribed to the cavitation induced rupture of microvessels and the secondary inflammation, leading to the initiation of angiogenesis. This study aimed to use ultrasound and microbubble to treat low limb ischemia in DM mice, and observe whether ultrasound-induced microbubble cavitation may promote angiogenesis and further explore the potential mechanism.

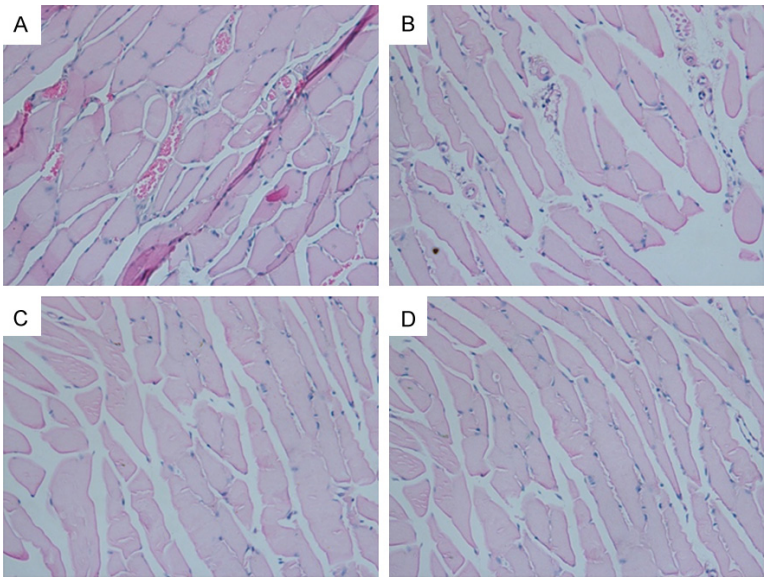

Figure 1. H&E staining of the skeletal muscle. A. US+MB group: there were a lot of red blood cells leaking into skeletal tissues, and the muscle fibers showed mild edema; B. US group: hemolysis was observed in a few vessels and there were no leaking red blood cells; C. MB group: there were no vascular congestion and leaking red blood cells; D. Control group: there were no vascular congestion and no leaking red blood cells.

Materials and methods

Materials

Male db/db mice aged 8-10 weeks were purchased from the Nanjing Model Experimental Animal Center. SonoVue ultrasound contrast agent (Bracco, Italy) was mixed with 5 ml of normal saline before used. The microbubbles were 2.5 μm in diameter and their concentration was 5×10^8/ml. PHYSIOSON Expert Therapeutic Portable Ultrasound Device (PHYSIOMED, Germany) was used in this study.

Animals

This study was approved by the Ethics Committee of Tongji Hospital, Tongji University. Mice received food deprivation for 12 h before surgery, but were given *ad libitum* access to water. The skin was prepared at the proximal skeletal muscle of the lower limb. Mice were intraperitoneally anesthetized with 1% sodium pentobarbital at 30 mg/Kg, and then placed on a table in a supine position. After disinfection, an incision was made at the middle of the knee of right low limb vertical to the inguinal ligament. The fascias and muscles were sequentially separated, and hemostasis was done by pressurization. The femoral vein and artery were separated under a microscope, and both were ligated at the distal end of the iliac artery bifurcation at two sites and then cut between them. The wound was closed, and buprenorphine hydrochloride was used after surgery for pain relief.

Methods

At 3 days after surgery, mice were randomly assigned into 4 groups: ultrasound+microbubble (US+MB) group (n=10) (mice were injected with 0.1 ml of SonoVue via the tail vein, and ultrasound was used at the skeletal muscle; coupling agent was smeared at the right groin, the frequency of probe was 1 MHz, the power was 2 W, duty cycle was 20%, and ultrasound was used for 2 min), US group (n=10; only ultrasound was used at the skeletal muscle), MB group (n=10; mice were injected with 0.1 ml of SonoVue via the tail vein) and control group (n=10). After ultrasound treatment, 3 mice in each group were sacrificed, and the right lower limb was harvested for H&E staining. Seven days later, remaining mice were sacrificed and the right lower limb was collected for RT-PCR and Western blot assay for the detection of mRNA and protein expressions of P-selectin, intercellular adhesion molecular (ICAM)-1 and vascular endothelial growth factor (VEGF) and immunohistochemistry for VEGF.

Real time PCR

Total RNA was extracted with Trizol reagent and cDNA was synthesized by reverse transcription with RevertAIDTM First Strand cDNA Synthesis (TAKARA, JAPAN). PCR was performed 7500 fluorescence quantitative PCR instrument. The conditions for PCR were as follows: 45 cycles of 95°C for 30 s, 95°C for 5 s and 60°C for 34 s. The experiment was repeated three times. The mRNA expression of ICAM-1, P-selectin and VEGF was detected, and GAPDH served as a control. Primers were synthesized in BGI biotech Co., Ltd.

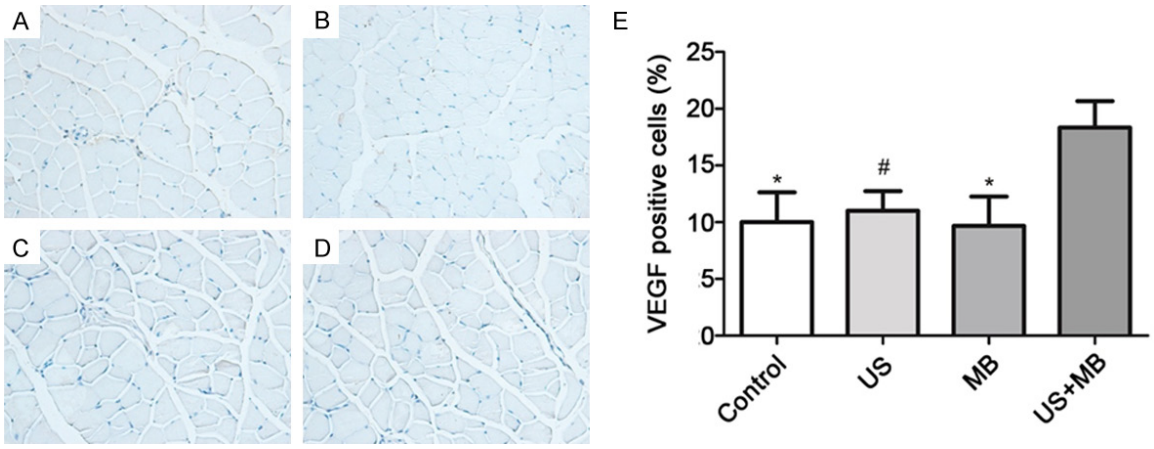

Figure 2. Immunohistochemistry for VEGF expression in different groups. A. US+MB group: VEGF expression was at a high level and the angiogenesis was active in the skeletal muscle; B. VEGF expression was at a low level in the skeletal muscle; C. VEGF expression was at a low level, and there were no newly generated vessels in the skeletal muscle; D. Control group: VEGF expression was at a low level, and there were no newly generated vessels in the skeletal muscle; E. Quantification of VEGF expression in the skeletal muscle. *P<0.01 vs. US+MB group; #P<0.05 vs. US+MB group.

Western blot assay

At 7 days after surgery, the skeletal muscle was collected for the detection of protein expression of ICAM-1, P-selectin and VEGF. Protein extraction: 100 mg of skeletal muscle was mixed with 0.5 ml of RIPA lysis buffer and homogenized for 5 min at 4°C. After centrifugation at 12000 g for 5 min, the supernatant was harvested, and protein concentration was determined with BCA method. The supernatant was stored at -80°C. SDS-PAGE: The protein was loaded, and electrophoresis was done in 5% stack gel at 80 V for 30 min and then in 8% separating gel at 110 V for 100 min. Transferring, hybridization and visualization: Proteins were transferred onto PVDF membrane at 4°C for 3 h at a constant current (0.25 A). The membrane was blocked in 7% BSA-TBST (25 mM Tris, 137 mM NaCl, 2.7 mM KCl and 0.1% Tween 20) for 1 h. After washing in TBST thrice, the membrane was incubated with primary antibody in 5% BSA-TBST at 4°C for 12 h. After washing in TBST 4 times (15 min for each), the membrane was treated with HRP conjugated secondary antibody in 5% BSA-TBST at room temperature for 1 h. Following washing in TBST 4 times (15 min for each), visualization was done. Image J software was employed to detect the optical density of each band. The expression of target protein was normalized to that of GAPDH.

Immunohistochemistry for VEGF

The skeletal muscle was fixed in 4% paraformaldehyde, embedded in paraffin, sectioned and subjected to H&E staining. Immunohistochemistry was performed with SABC method according to manufacturer's instructions. After visualization with DAB and counterstaining with hematoxylin, sections were observed under a light microscope. Positive cells had brown granules. In the negative control group, the primary antibody was replaced with PBS. The VEGF expression was semi-quantified with Image J software. Five fields were randomly selected from each section at 200×, and the integrated optical density (IOD) was determined.

Statistical analysis

All the data are expressed as mean ± standard deviation. Statistical analysis was performed with SPSS version 19.0. Qualitative data were compared with chi square test, and quantitative data with one way analysis of variance, followed by Bonferroni test for intragroup comparison. A value of two-tailed $P<0.05$ was considered statistically significant.

Results

H&E staining of the skeletal muscle

In US+MB group, there were a lot of red blood cells leaking, the muscle fibers showed mild

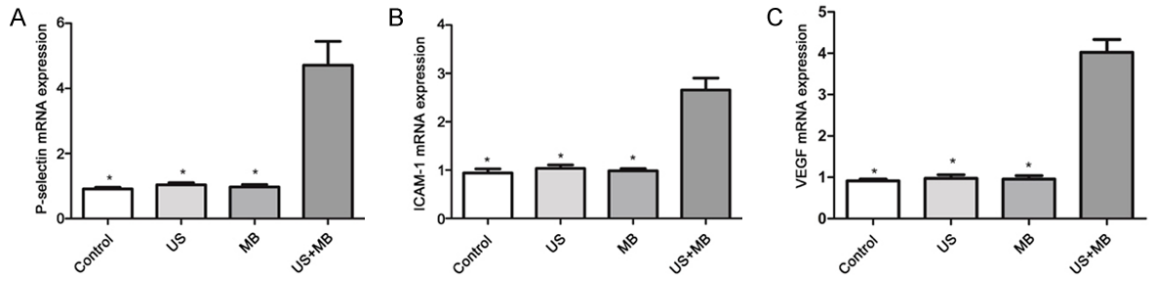

Figure 3. Expression of P-selectin (A), ICAM-1 (B) and VEGF (C) in different groups. *P<0.01 vs US+MB group.

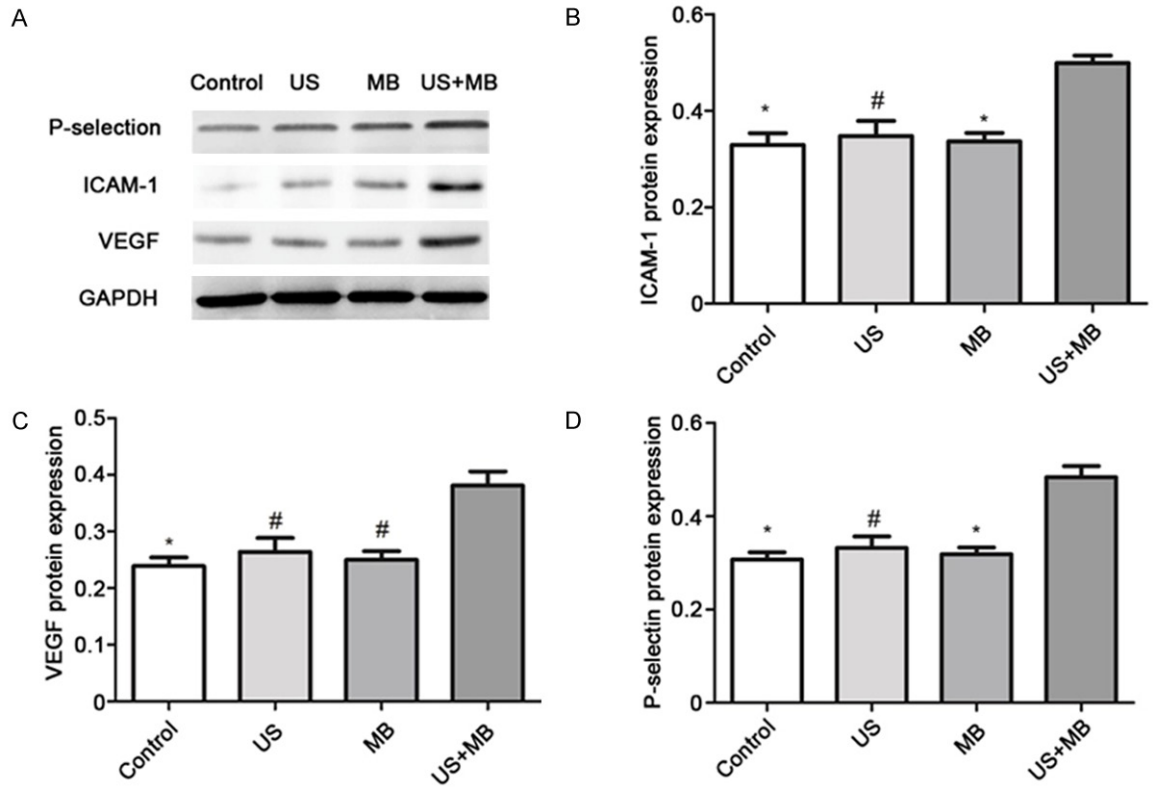

Figure 4. Protein expressions of ICAM-1, VEGF and P-selectin in the skeletal muscle. A. Western blot assay; B. ICAM-1 protein expression. C. VEGF protein expression. D. P-selection protein expression. *P<0.01 vs US+MB group; #P<0.05 vs US+MB group.

edema and there was no myolysis (**Figure 1A**). In US group, hemolysis was found in a few vessels, and red blood cells leaking into skeletal muscle gap and skeletal muscle injury were not observed (**Figure 1B**). In MB group and control group, there were no vascular congestion and leaking red blood cells (**Figure 1C** and **1D**).

Immunohistochemistry for VEGF

In US+MB group, the VEGF expression was at a high level, and a lot of newly generated blood vessels were observed (**Figure 2A**). In US group (**Figure 2B**), MB group (**Figure 2C**) and control group (**Figure 2D**), the VEGF expression was at a low level. **Figure 2E** showed the VEGF expression in US+MB group was significantly higher than in control group, MB group (P<0.01) and US group (P<0.05).

Real time RT-PCR

Real time RT-PCR showed the mRNA expression of P-selectin was the highest in US+MB group and significantly higher than in other groups (P<0.01) (**Figure 3A**). The mRNA expres-

sion of ICAM-1 in US+MB group was the highest and markedly higher than in other groups (P<0.01) (**Figure 3B**). The mRNA expression of VEGF was the highest in US+MB group and significantly higher than in other groups (P<0.01) (**Figure 3C**).

Western blot assay

As shown in **Figure 4A**, the protein expression of ICAM-1 in US+MB group was significantly higher than in control group, MB group (P<0.01) and US group (P<0.05). As shown in **Figure 4B**, the protein expression of VEGF in US+MB group was markedly higher than in control group (P<0.01), US group and MB group (P<0.05). As shown in **Figure 4C**, the protein expression of P-selection in US+MB group was significantly higher than in control group, MB group (P<0.01) and US group (P<0.05).

Discussion

It has been accepted that ultrasound may induce the microbubble cavitation. Microbubble ultrasound contrast agents may serve as effective cavitation nuclei [3]. In case of cavitation, the microbubbles may cause mechanical injury to the surrounding cells and tissues and produce potential biological consequences. Ultrasound-mediated microbubble destruction and sonoporation may cause "ultrasonic drilling" effect [5, 7], which is usually accompanied by two phenomena: a group of microbubbles may serve as artificial cavitation nuclei, which may reduce the energy threshold required for the ultrasound-mediated microbubble cavitation, enhance the sonoporation and further increase the permeability of cell membrane; the gap between endothelial cells is widened, and drugs or genes may enter the tissues or cells via the ruptured microvessels and the gap, leading to the targeted transportation. In addition, ultrasound on the microbubble may induce local inflammation, in which a lot of inflammatory cells aggregate and a variety of inflammatory cytokines are released, resulting in a series of potential biological effects [8, 9].

A majority of investigators speculate that ultrasound and microbubbles induced angiogenesis is related to the elevated expression of VEGF and bFGF secondary to the release of inflammation after the damage to the local vascular endothelial cells [10, 11]. Our results showed the mRNA and protein expressions of VEGF in US+MB group were significantly higher than in US group, MB group and control group, which confirms that the elevated VEGF expression is as a result of ultrasound induced microbubble cavitation. The ultrasound induced microbubble cavitation may cause the increase in the permeability of capillaries in the skeletal muscle. H&E staining showed there were a lot of red blood cells leaking into the muscle gap in US+MB group. In US group, hemolysis was found in only a few vessels, and there were no leaking red blood cells and skeletal muscle injury. These findings indicate that the action of ultrasound on microbubbles causes the rupture of microvessles as well as the leakage of red blood cells into tissues. In addition, some inflammatory cells infiltrated into the ischemic skeletal muscle, and the expression of P-selectin and ICAM-1 in US+MB group was significantly higher than in US group, MB group and control group. P-selectin, ICAM-1 and VCAM-1 are involved in the adhesion, aggregation and exudation of leukocytes, and excess expression of these cytokines may mediate the infiltration of inflammatory cells and immune cells. P-selectin is a receptor on the neutrophils and monocytes and can recognize the specific oligosaccharide structure on cells. It is stored in the platelet α particles and endothelial Weibel-Palade body. As a response to stimulation, these cells may express P-selectin within several minutes, inducing the activation of endothelial cells. This process initiates the adhesion of leukocytes in the acute inflammation. The high expression of P-selectin on the endothelial cells may induce the rolling and adhesion of inflammatory cells including neutrophils, resulting in the inflammatory cascade [12-14]. ICAM-1 has been regarded as a factor mediating the intercellular adhesion. Under normal conditions, ICAM-1 expression is at a low level on leukocytes and endothelial cells. However, in case of inflammation, ICAM-1 is highly expressed, but the production of ICAM-1 is later than that of P-selectin. ICAM-1 may recognize and anchor inflammatory cells, and facilitate and stabilize the intercellular adhesion, which play crucial roles in the infiltration of leukocytes into the inflammatory sites. In our study, the protein and mRNA expressions of P-selectin and ICAM-1 in US group were significantly higher than in US group, MB group and control group. Thus, we postulate that the action of ultrasound in the presence of microbubbles may induce the expression of pro-

inflammatory cytokines (P-selectin and ICAM-1) to facilitate the infiltration of inflammatory cells and the expression of VEGF, leading to the angiogenesis. These findings were consistent with those reported by Song et al [6].

Taken together, ultrasound in the presence of microbubbles may induce mild damage to the endothelial cells in the capillaries of local interstitium and cause transient inflammation, which then lead to the activation of endothelial cells and up-regulate the expression of P-selectin and ICAM-1, resulting in the elevated synthesis of VEGF and subsequence angiogenesis in the ischemic skeletal muscle. The ultrasound induced destruction of microbubbles may serve as a new method for the therapeutic angiogenesis in the ischemic skeletal muscles in DM patients. Of note, this fails to improve the nutritional blood flow for a long time, and thus it efficacy is limited. In our future study, US+MB will be combined with stem cells transplantation or gene transfection for the improvement of local blood flow and angiogenesis.

Acknowledgements

This study was supported by the Capacity Building Project of Clinical Ancillary Departments (SHDC: 22015009).

Disclosure of conflict of interest

None.

Address correspondence to: Peijun Wang, Department of Radiology, Affiliated Tongji Hospital of Tongji University, Shanghai 200065, China. Tel: +8621-6611292; E-mail: tongjipjwang@vip.sina.com

References

[1] Forsythe RO and Hinchliffe RJ. Management of peripheral arterial disease and the diabetic foot. J Cardiovasc Surg (Torino) 2014; 55: 195-206.

[2] Park B, Hoffman A, Yang Y, Yan J, Tie G, Bagshahi H, Nowicki PT and Messina LM. Endothelial nitric oxide synthase affects both early and late collateral arterial adaptation and blood flow recovery after induction of hind limb ischemia in mice. J Vasc Surg 2010; 51: 165-173.

[3] Liu J, Zhang P, Liu P, Zhao Y, Gao S, Tan K and Liu Z. Endothelial adhesion of targeted microbubbles in both small and great vessels using ultrasound radiation force. Mol Imaging 2012; 11: 58-66.

[4] Miller DL, Averkiou MA, Brayman AA, Everbach EC, Holland CK, Wible JH Jr and Wu J. Bioeffects considerations for diagnostic ultrasound contrast agents. J Ultrasound Med 2008; 27: 611-632; quiz 633-616.

[5] Zha Z, Wang S, Zhang S, Qu E, Ke H, Wang J and Dai Z. Targeted delivery of CuS nanoparticles through ultrasound image-guided microbubble destruction for efficient photothermal therapy. Nanoscale 2013; 5: 3216-3219.

[6] Song J, Cottler PS, Klibanov AL, Kaul S and Price RJ. Microvascular remodeling and accelerated hyperemia blood flow restoration in arterially occluded skeletal muscle exposed to ultrasonic microbubble destruction. Am J Physiol Heart Circ Physiol 2004; 287: H2754-2761.

[7] Nofiele JT, Karshafian R, Furukawa M, Al Mahrouki A, Giles A, Wong S and Czarnota GJ. Ultrasound-activated microbubble cancer therapy: ceramide production leading to enhanced radiation effect in vitro. Technol Cancer Res Treat 2013; 12: 53-60.

[8] Kobulnik J, Kuliszewski MA, Stewart DJ, Lindner JR and Leong-Poi H. Comparison of gene delivery techniques for therapeutic angiogenesis ultrasound-mediated destruction of carrier microbubbles versus direct intramuscular injection. J Am Coll Cardiol 2009; 54: 1735-1742.

[9] Mayer CR and Bekeredjian R. Ultrasonic gene and drug delivery to the cardiovascular system. Adv Drug Deliv Rev 2008; 60: 1177-1192.

[10] Fujiyama S, Amano K, Uehira K, Yoshida M, Nishiwaki Y, Nozawa Y, Jin D, Takai S, Miyazaki M, Egashira K, Imada T, Iwasaka T and Matsubara H. Bone marrow monocyte lineage cells adhere on injured endothelium in a monocyte chemoattractant protein-1-dependent manner and accelerate reendothelialization as endothelial progenitor cells. Circ Res 2003; 93: 980-989.

[11] Chappell JC, Song J, Klibanov AL and Price RJ. Ultrasonic microbubble destruction stimulates therapeutic arteriogenesis via the CD18-dependent recruitment of bone marrow-derived cells. Arterioscler Thromb Vasc Biol 2008; 28: 1117-1122.

[12] Carr CL, Qi Y, Davidson B, Chadderdon S, Jayaweera AR, Belcik JT, Benner C, Xie A and Lindner JR. Dysregulated selectin expression and monocyte recruitment during ischemia-related vascular remodeling in diabetes mellitus. Arterioscler Thromb Vasc Biol 2011; 31: 2526-2533.

[13] Lindner JR, Song J, Christiansen J, Klibanov AL, Xu F and Ley K. Ultrasound assessment of inflammation and renal tissue injury with microbubbles targeted to P-selectin. Circulation 2001; 104: 2107-2112.

[14] Kaufmann BA, Lewis C, Xie A, Mirza-Mohd A and Lindner JR. Detection of recent myocardial ischaemia by molecular imaging of P-selectin with targeted contrast echocardiography. Eur Heart J 2007; 28: 2011-2017.